

**Title: MOLECULAR DETERMINANTS IN THE SECOND INTRACELLULAR LOOP OF THE 5-HYDROXYTRYPTAMINE(1A) (5-HT1A) RECEPTOR FOR G-PROTEIN COUPLING<sup>1</sup>**

**Authors:** Neena Kushwaha, Shannon C. Harwood, Ariel M. Wilson, Miles Berger<sup>#</sup>, Laurence H. Tecott<sup>#</sup>, Bryan L. Roth<sup>##</sup> and Paul R. Albert<sup>\*</sup>

Ottawa Health Research Institute (Neuroscience) and Department of Cellular and Molecular Medicine, University of Ottawa, 451 Smyth Road, Ottawa, Ontario, Canada K1H 8M5;

<sup>#</sup>Department of Psychiatry, Center for Neurobiology and Psychiatry, Institute for Neurodegenerative Diseases, University of California, San Francisco School of Medicine, San Francisco, CA 94143.

<sup>##</sup>Department of Biochemistry, Case Western Reserve University Medical School, Cleveland, OH 44106

**Running Title: Coupling of 5-HT<sub>1A</sub>-i<sub>2</sub> mutant receptors**

Neena Kushwaha, Shannon C. Harwood, Ariel Wilson, Miles Berger, Laurence H. Tecott, Bryan L. Roth and Paul R. Albert\*

Ottawa Health Research Institute (Neurosciences) and Department of Cellular and Molecular Medicine, University of Ottawa, 451 Smyth Road, Ottawa, Ontario, Canada K1H 8M5

\*Corresponding author: Ottawa Health Research Institute (Neurosciences), 451 Smyth Road, Ottawa, Ontario, Canada, K1H 8M5; Phone: (613) 562-5800 x-8307; Fax: (613) 562-5403; Email: [palbert@uottawa.ca](mailto:palbert@uottawa.ca).

Number of text pages: 33

Number of tables: 2

Number of figures: 3

Number of references: 39

Number of words in Abstract: 253

Number of words in Introduction: 782

Number of words in Discussion: 1119

**ABBREVIATIONS:** cAMP, cyclic adenosine monophosphate; Ci<sub>2</sub>, C-terminal of the i<sub>2</sub> loop; Ci<sub>3</sub>, C-terminal of the i<sub>3</sub> loop; 8-OH-DPAT, 8-hydroxy-2-(di-n-propylamino)tetralin; EDTA, ethylenediaminetetraacetic acid; ERK1/2, extracellular regulated kinases 1 and 2; GRK-CT, C-tail of G protein receptor kinase 2; IBMX, 3-isobutyl-1-methylxanthine; MAPK, mitogen activated protein kinase; MEK1/2, MAP/ERK kinases 1 and 2; MUG, 4-methylumbelliferyl- $\beta$ -D-galactosidase; Ni<sub>2</sub>, N-terminal of the i<sub>2</sub> loop; Ni<sub>3</sub>, N-terminal of the i<sub>3</sub> loop.

## ABSTRACT

This study provides the first comprehensive evidence that the second intracellular loop C-terminal domain (Ci2) is critical for receptor–G protein coupling to multiple responses. Although Ci2 is weakly-conserved, its role in 5-HT1A receptor function was suggested by the selective loss of G $\beta\gamma$ -mediated signaling in the T149A-5-HT1A receptor mutant. Over sixty point mutant 5-HT1A receptors in the alpha-helical Ci2 sequence (<sup>143</sup>DYVNKRTPRR<sup>152</sup>) were generated. Most mutants retained agonist binding and were tested for G $\beta\gamma$  signaling to adenylyl cyclase II or phospholipase C and G $\alpha_i$  coupling, to detect constitutive and agonist-induced Gi/Go coupling. Remarkably, most point mutations markedly attenuated 5-HT1A signaling, indicating that the entire Ci2 domain is critical for receptor G-protein coupling. Six signaling phenotypes were observed: wild-type-like; G $\alpha_i$ -coupled/weak G $\beta\gamma$ -coupled; G $\beta\gamma$ -uncoupled; G $\beta\gamma$ -selective coupled; uncoupled; and inverse coupling. Our data elucidate specific roles of Ci2 residues consistent with predictions based on rhodopsin crystal structure. The absolute coupling requirement for lysine, arginine, and proline residues is consistent with a predicted amphipathic alpha-helical Ci2 domain that is kinked at Pro150. Polar residues (T149, N146) located in the externally-oriented positively-charged face were required for G $\beta\gamma$  but not G $\alpha_i$  coupling, suggesting a direct interface with G $\beta\gamma$  subunits. The hydrophobic face includes the critical Y144 that directs the specificity of coupling to both G $\beta\gamma$  and G $\alpha_i$  pathways. The key coupling residues Y144/K147 (Ci2) are predicted to orient internally, forming hydrogen and ionic bonds with D133/R134 (Ni2 DRY motif) and E340 (Ci3) to stabilize the G-protein coupling domain. Thus, the 5-HT1A receptor Ci2 domain determines G $\beta\gamma$  specificity and stabilizes G $\alpha_i$ -mediated signaling.

## INTRODUCTION

The receptor domains that mediate coupling to  $G\alpha$ -induced responses have been intensively studied, but determinants of  $G\beta\gamma$  signaling have yet to be addressed (Bourne, 1997; Meng and Bourne, 2001; Sakmar et al., 2002). Deletion and point mutagenesis studies have indicated that the N- and C-terminal portions of the i3 domain (Ni3, Ci3) as well as i2 and C-terminal regions play important roles in receptor coupling to G-proteins (Shapiro et al, 2002). Using a saturation mutagenesis approach to study the Gq-coupled m5-muscarinic receptor, the i2 and Ni3 domains were predicted to form an amphipathic alpha-helical structure with charged residues of Ni3 recruiting G-proteins to form interactions with embedded hydrophobic residues (Burstein et al., 1996; Burstein et al., 1998; Hill-Eubanks et al., 1996). Similarly, saturation and cysteine mutagenesis of the Ci3 domain (near TMIV) suggests an alpha-helical structure containing residues that interact with G-protein and intracellular receptor domains to regulate constitutive activity (Liu et al., 1995; Schmidt et al., 2003; Shi et al., 2002; Spalding et al., 1998; Zeng et al., 1999). The crystal structure of cis-retinal-bovine rhodopsin (inactive state) (Palczewski et al., 2000) has revealed some intramolecular interactions that are thought to lock the receptor in an inactive state, especially between the conserved (D/E)RY motif at TM3/Ni2 and a conserved D/E residue of Ci3/TM6 (Ballesteros et al., 2001; Meng and Bourne, 2001; Zeng et al., 1999; Shapiro et al, 2002; Shapiro et al., 2002). Although the importance of the conserved (D/E)RY motif in the Ni2 region in receptor activation has been examined extensively (Meng and Bourne, 2001; Sakmar et al., 2002), the structure and importance of the adjacent Ci2 domain in coupling has yet to be addressed. Random mutagenesis of the m5-muscarinic i2 domain yielded few functional mutants of the Ci2 region (Burstein et al., 1998), suggesting the potential importance this domain in coupling. However, their  $G\alpha_q$ -mediated signaling screen did not select nonfunctional

mutants, hence no firm conclusion could be reached regarding Ci2 function. Furthermore, previous receptor mutagenesis studies have not addressed G $\beta\gamma$ -mediated signaling, which increasing evidence suggests can be dissociated from G $\alpha$ -mediated coupling (Albert and Robillard, 2002; Chidiac, 1998).

Hence, we have examined in detail the role of the Ci2 domain in 5-HT1A receptor coupling to both G $\alpha_i$  and G $\beta\gamma$ -mediated signaling pathways. The 5-HT1A receptor is a Gi/Go-coupled receptor that is a critical regulator of the brain serotonergic system and has been implicated in mental illnesses such as depression and anxiety (Albert and Lemonde, 2004; Gross and Hen, 2004; Pineyro and Blier, 1999). In previous studies we found that mutation of a single threonine residue (Thr149Ala) within the Ci2 region, reduced or blocked 5-HT1A receptors from coupling to several G $\beta\gamma$ -mediated pathways, but not to G $\alpha_i$ -mediated inhibition of forskolin or Gs-stimulated adenylyl cyclase activation (Albert et al., 1998; Lembo et al., 1997; Liu et al., 1999). The affected G $\beta\gamma$  pathways included: phospholipase C-mediated calcium mobilization (Kushwaha and Albert, 2005; Lembo et al., 1997; Wurch et al., 2003); inhibition of dihydropyridine-induced (L-type) and N-type calcium channel activation (Lembo et al., 1997; Wu et al., 2002); and constitutive activation of adenylyl cyclase II (Albert et al., 1999). The T149A mutation also blocked 5-HT1A-mediated MAPK inhibition in raphe RN46A cells (Kushwaha and Albert, 2005). Thus, the T149A residue of the Ci2 domain plays a crucial role in G $\beta\gamma$ -induced pathways of the 5-HT1A receptor. In addition to the i2 domain, the i3 and palmitoylated C-terminal domains of the 5-HT1A receptor have also been implicated in G-protein coupling (Papoucheva et al., 2004; Sun and Dale, 1999; Turner et al., 2004; Varrault et al., 1994). Peptides derived from the Ni3 or Ci3 domains of the 5-HT1A receptor can mimic G $\alpha_i$ -mediated inhibition of adenylyl cyclase, while i2 peptides prevented this coupling (Ortiz et

al., 2000; Varrault et al., 1994). This suggests that Ni3 and Ci3 domains may mediate activation of G $\alpha$ i, while the i2 loop is involved in receptor interaction with G $\alpha$ i, but not its activation.

Computer-based analysis predicts that the Ci2 domain has an amphipathic alpha-helical structure that is conserved among many G-protein coupled receptors (GPCRs) (Albert et al., 1998). In order to provide insight into the structural determinants of the Ci2 loop and empirical validation of their importance for 5-HT1A receptor coupling to G-protein signaling, we have generated a series of random targeted point mutants of nine critical i2 residues that are predicted to form the amphipathic  $\alpha$ -helical domain. Based on the coupling of tolerated substitutions we have used computer modeling to identify critical amino acid side-chain interactions that are implicated in G $\alpha$ i and G $\beta\gamma$  signaling of the receptor. Using this approach we have provided the first comprehensive insights into the role of the Ci2 domain in both G $\alpha$  and G $\beta\gamma$  signaling.

## Materials and Methods

**Materials.** All chemicals were reagent grade. Forskolin, IBMX, MUG, 5-HT, pertussis toxin, EGTA, and 8-OH-DPAT were purchased from Sigma (St. Louis, MO). Fura-2-AM was obtained from Molecular Probes (Eugene, OR). [<sup>125</sup>I]-succinyl cAMP (2200 Ci/mmol) was purchased from NEN Life Science Products (Boston, MA). Anti-3', 5'-cAMP antibody was obtained from ICN Biomedicals, Inc. (Aurora, Ohio). The QuikChange™ XL Site-Directed Mutagenesis Kit was obtained from Stratagene (La Jolla, CA).

**Plasmids.** To generate the 5-HT1A expression plasmids a 1.9 kb BamHI/XbaI fragment of the rat 5-HT1A receptor gene wild-type (1A) or receptor mutant (T149A-i2) were subcloned into BamHI/XbaI-digested pcDNA3 (Invitrogen). For construction of 5-HT1A-i2 mutant receptors, single point mutations of each amino acid in the 5-HT1A-i2 loop sequence DYVNKRTPRR were generated randomly using a primer-directed mutagenesis kit (QuikChange™ XL Site-Directed Mutagenesis Kit, Stratagene). For example, to generate 5-HT1A receptors mutated at T149 the following oligonucleotides were used, Sense: 5'-TATAGACTATGTGAACAAAAGG NNGCCCCGG-3' and Antisense: 5'-CGCGCCGGGGCNNCCTTTTGTTACATAGTC-3'. Mutant primers used for each i2 loop residue are listed in the *Supplemental Table 1*. Using the wild-type 5-HT1A cDNA (described above) as template, we prepared the sample reactions according to the manufacturer's protocol and used the recommended cycling parameters to amplify PCR products. The receptor mutants were identified using Sanger dideoxynucleotide termination DNA sequencing method with the following primer located 40-80 nucleotides adjacent to the sites of the mutation, 5'-CTGTGCTGCACCTCGTCCATCCTG-3'.

**Cell Culture and Transfection.** Human embryonic kidney (HEK) 293 cells were maintained in DMEM (Wisent) + 7% fetal bovine serum (FBS) (Invitrogen) at 37°C in 5% CO<sub>2</sub>. HEK 293 cells were plated at 7 X 10<sup>6</sup> cells/10-cm dish and incubated overnight. For measurement of constitutive 5-HT<sub>1A</sub> receptor activity, cells were transiently transfected by calcium phosphate co-precipitation with 12 µg each of the indicated plasmids (adenylyl cyclase II, Gαi2, and 5-HT<sub>1A</sub>-wt or 5-HT<sub>1A</sub>-i2 mutant receptor), and 6 µg of pCMV-βGAL in 7 ml/dish DMEM + 10% FCS, 20 mM Hepes (pH 7.0) at 37°C (5% CO<sub>2</sub>) for 4-6 h. Consistent basal cAMP levels were observed between wt and mutant receptors indicating similar levels of adenylyl cyclase II expression between transfections. To measure the inhibition of dopamine-stimulated cAMP formation by 5-HT<sub>1A</sub> receptor activation, HEK 293 cells were transiently transfected with 12 µg of both the human dopamine-D1 and rat 5-HT<sub>1A</sub> receptors. The cells were then plated onto 6-well plates for cAMP and β-galactosidase assays. Consistent dopamine responses were obtained amongst wt and mutant receptors indicating equivalent expression levels of the D1 receptor coupling between transfections. Ltk- cells were cultured in α-MEM (Wisent) supplemented with 5% FBS at 37°C (5% CO<sub>2</sub>). For intracellular calcium measurements Ltk- cells were transiently transfected with 5 µg of either 5-HT<sub>1A</sub>-wt or 5-HT<sub>1A</sub>-i2 mutant receptors using Lipofectamine Plus reagents (Invitrogen) according to the manufacturer's protocol. Cells were harvested after 48 hrs for intracellular calcium measurements. In parallel experiments, membranes were prepared from Ltk- cells transiently transfected with the indicated 5-HT<sub>1A</sub> mutant receptors and subjected to binding analysis with [<sup>3</sup>H]-OH-DPAT.



**cAMP Assay.** Measurement of cAMP was performed as described previously (Albert et al., 1998). Briefly, 24 h after plating HEK cells into 6-well dishes, the cells were washed once with serum-free DMEM and incubated in 1 ml/well of DMEM, 20 mM N-2-hydroxyethylpiperazine-N9-2-ethanesulfonic acid (pH 7.0), 100  $\mu$ M IBMX for 15-20 min at 37°C. Experimental compounds were added to triplicate wells as indicated. Media were collected, centrifuged at 14,000 X g (30 s) to remove floating cells, and the supernatant was stored at -20°C until assayed for cAMP using a specific radioimmunoassay (ICN) as described (Albert et al., 1998). Attached cells were harvested using reporter lysis buffer (Promega), centrifuged for 2 min at 4°C, and stored at -20°C. Transfection efficiency was monitored by cotransfection of  $\beta$ -galactosidase plasmid and cAMP values were normalized to  $\beta$ -gal activity (Albert et al., 1999). Pertussis toxin (50 ng/ml) was present overnight (16h) in indicated samples.

**$\beta$ -Galactosidase Assay.** Transfection efficiencies were monitored by  $\beta$ -galactosidase assay. The transfected cells were rinsed with PBS, resuspended in 200  $\mu$ l of reporter lysis buffer, incubated for 15 min at room temperature, scraped, frozen, and thawed to complete cell lysis. The lysates were centrifuged (14,000 rpm, 2 min, 4°C) and the supernatant was recovered for measurement of  $\beta$ -galactosidase activity. Equal volumes (30  $\mu$ l each) of cell extract and 0.3 mM MUG substrate in 15 mM Tris (pH 8.8) were mixed gently, incubated in the dark at 37°C for 30 min, and the reaction was terminated upon addition of 50  $\mu$ l of Stop solution (300 nM glycine, 15 mM EDTA pH 11.2). The sample was transferred to 2 ml of Z buffer (60 mM Na<sub>2</sub>HPO<sub>4</sub>, 40 mM NaH<sub>2</sub>PO<sub>4</sub>, 10 mM KCl, 1 mM MgSO<sub>4</sub>), and the fluorescence was measured at  $\lambda_{EX} = 350$ nm,  $\lambda_{EM} = 450$  nm on a Perkin-Elmer LS-50 spectrofluorometer (Buckinghamshire, United

Kingdom). The average  $\beta$ -galactosidase activity for transfection of mutant receptor plasmids in each experiment ranged from 0.8-1.3-fold of that for wild-type receptor.

**Ligand Binding.** Cell membranes were prepared from transfected cultures on 15-cm dishes by replacing the growth medium with ice-cold hypotonic buffer (15 mM Tris-HCl, pH 7.4, 2.5 mM MgCl<sub>2</sub>, 0.2 mM EDTA). After swelling for 10-15 min at 4°C, the cells were scraped from the plates, sonicated on ice, centrifuged (14,000 rpm for 20 min) and resuspended in ice-cold TME buffer (75 mM Tris-HCl, pH 7.4, 12.5 mM MgCl<sub>2</sub>, 1 mM EDTA). Aliquots of thawed and sonicated membrane preparation (100  $\mu$ g/tube) were added to triplicate tubes containing 200  $\mu$ l TME and 10 nM [<sup>3</sup>H]-8-OH-DPAT (Amersham) without or with 5-HT (10  $\mu$ M) to determine total vs. non-specific binding at room temperature (30 min). Reactions were terminated by filtration through GF/C (Whatman) filters, washing with 3 x 4 ml of ice-cold buffer (50 mM Tris-HCl, pH 7.4) and 3 ml of scintillation fluid added to filters to quantify radioactivity by liquid scintillation counting. Protein was assayed with the BCA protein assay kit (Pierce) with bovine serum albumin as a standard.

**Measurement of Intracellular Calcium.** As described previously (Liu and Albert, 1991), cells were grown to 80% confluence, harvested with trypsin/EDTA, resuspended in 3 ml of serum-free DMEM with the calcium indicator Fura-2 AM (3  $\mu$ M), and incubated for 30 min at 37°C with shaking (100 rpm). The cells were washed once with HBBS-Ca<sup>2+</sup> (pH 7.4), resuspended in 2 ml of buffer, and subjected to fluorometric measurement. Changes in fluorescence ratio was recorded on a Perkin-Elmer Cetus (Buckinghamshire, UK) LS-50 spectrofluorometer and analyzed by computer, based on a K<sub>d</sub> value of 227 nM for the Fura-2/Ca<sup>2+</sup> complex. Calibration

of  $R_{\max}$  was performed by the addition of 0.1% Triton X-100 and 20mM Tris base and of  $R_{\min}$  by the addition of 10mM EGTA. Experimental compounds were added directly to cuvette at the specified concentrations at the indicated times.

**Statistical Analysis.** The data are presented as mean  $\pm$  SEM of at least three independent experiments. Statistical analyses of the data were done using GraphPad Prism software (San Diego, CA).

**Modeling.** A preliminary model of the rat 5-HT<sub>1A</sub> receptor (inactive state) was prepared using bovine rhodopsin as template using methodology similar to that described previously (Setola et al, 2005; Shapiro et al, 2002). The full details of the model will be described in a subsequent publication.

## RESULTS

*Mutagenesis strategy.* We employed a random primer-based mutagenesis approach to incorporate point mutations targeted at the 5-HT1A-i2 loop sequence <sup>143</sup>DYV NKRTPRR<sup>152</sup>, a region implicated in G-protein coupling of the receptor (Albert et al., 1998). The function of mutant receptors was examined using three rapid functional assays in transiently transfected cells: coupling to adenylyl cyclase II or to phospholipase C $\beta$  (both G $\beta\gamma$ -mediated); or inhibition of Gs-stimulated adenylyl cyclase activation (G $\alpha_i$ -mediated). Each of these 5-HT1A receptor-mediated signals is blocked by pertussis toxin treatment indicating an obligatory role for Gi/Go proteins. Constitutive coupling to adenylyl cyclase II was assessed in HEK-293 cells cotransfected with 5-HT1A receptor, adenylyl cyclase II, and G $\alpha_i2$ , which results in an agonist-independent increase in cAMP that is mediated by G $\beta\gamma$  signaling and is reduced in the T149A 5-HT1A receptor mutant (Albert et al., 1999) (Fig. 1A). In this model addition of agonist does not increase cAMP any further, hence constitutive receptor coupling is measured. Agonist-mediated 5-HT1A receptor signaling to phospholipase C $\beta$  was assayed by measuring DPAT-induced calcium mobilization in transfected Ltk- fibroblast cells, a G $\beta\gamma$ -mediated pathway that is reduced by the T149A mutation (Lembo et al., 1997) (Fig. 2). Coupling of 5-HT1A receptors to G $\alpha_i$  (Liu et al., 1999) was examined by assaying agonist-mediated inhibition of Gs-stimulated (via D1 receptor) cAMP accumulation in transfected HEK-293 cells (Albert et al., 1999) (Fig. 1B).

*Mutant phenotypes.* Overall, 61 mutant receptors were generated and examined using the screening assays described above and these data are assembled in Table I. Most of the mutants displayed significant levels of specific binding (<sup>3</sup>H-DPAT) that was comparable to that of non-mutated 5-HT1A receptors (Table I). Some mutants displayed variation in binding levels due to

transfection efficiency, but all displayed at least one functional response except for one case (K147Q), indicating that these mutant receptors folded correctly and were functional. In addition the level of basal and dopamine-stimulated cAMP was similar in transfections of different mutants (data not shown), indicating consistent levels of adenylyl cyclase II or D1 receptor coupling among transfections. The majority (44/61) of the mutant receptors remained significantly coupled to  $G\alpha_i$ -mediated inhibition of cAMP accumulation (Table I).  $G\beta\gamma$ -signaling of mutant receptors, such as phospholipase  $C\beta$ -mediated calcium mobilization, was blocked by pertussis toxin (Fig. 2), indicating mediation by Gi/Go proteins. The mutant 5-HT1A receptors were classified into six main signaling phenotypes (Table II): wild-type-like (3/61, T149R,G; N146T);  $G\alpha_i$ -coupled/weak  $G\beta\gamma$ -coupled (8/61, T149AEQ; V145LK; R148G; R151AT);  $G\beta\gamma$ -uncoupled (16/61);  $G\beta\gamma$ -selective coupled (16/61); uncoupled (17/61); and a few mutants displayed inverse basal activity to inhibit adenylyl cyclase II (Fig. 1A) or mediated inverse agonist activity to potentiate D1-induced adenylyl cyclase activation (Fig. 1B). Only two mutants were identified (R152N/D) that lacked  $G\alpha_i$  coupling and retained minimal  $G\beta\gamma$  coupling, indicating an important role for the Ci2 domain in  $G\beta\gamma$  coupling. Within the  $G\beta\gamma$ -coupled group of receptors, signaling to adenylyl cyclase II or phospholipase C was selectively preserved depending on the mutation, and in several cases  $G\alpha_i$  signaling was also preserved (Table II). At other sites in the i2 domain most mutants were non-functional, suggesting that very few mutations preserve i2 structure required for proper G-protein coupling.

*Predicted structures.* Because 5-HT1A-i2 peptides mimic 5-HT1A receptor coupling to inhibition of adenylyl cyclase (Thiagaraj et al., 2002; Varrault et al., 1994) and trigger  $G\beta\gamma$ -mediated calcium mobilization (Kushwaha and Albert, unpublished) we examined the predicted

peptide secondary structures of the mutant Ci2 domains. The presence of a predicted amphipathic alpha-helical structure (Albert et al., 1998) was not altered by any of the point mutations of the Ci2 domain. Garnier-Robson analysis (Supplemental Table 2) revealed a predicted coil at T149/P150. Any mutant predicted to be disrupted, displaced or even reduced at the T149/P150 coil domain (T149AQWVM; all P150 mutants; V145KYES; N146A; R148LQV; R151AMLK; R152VA) displayed impaired coupling to G $\beta\gamma$  or both G $\alpha_i$  and G $\beta\gamma$  signaling (Table I). Strikingly, any substitution at residue Pro150 (Table I) completely disrupted of receptor function and was predicted to disrupt the predicted coil structure in the i2 peptide (Supplemental Table 2). Conversely, addition of a proline residue (e.g., R148P, T149P, R152P) resulted in weakly coupled receptors and an expanded coil domain. By contrast, the predicted hydrophobic alpha-helix at the start of TMIV (from R151-A155) was dispensable for coupling in the T149G/R mutants, while several mutants that lacked receptor signaling appeared to retain the TMIV alpha-helix. Thus the predicted coil structure at T149/P150 of the Ci2 domain appears to play a critical role 5-HT<sub>1A</sub> receptor signaling.

*Inverse Activity:* Several mutants displayed inverse activity (Fig. 1). The greatest inverse basal activity towards adenylyl cyclase II was observed for the R148K mutant receptor, which reduced cAMP levels to below that of pertussis toxin-treated samples, suggesting that the receptor inhibits the basal activity of adenylyl cyclase II (Fig. 1A). In Ltk- cells transfected with the R148K mutant, DPAT treatment did not alter basal or D1-induced cAMP, indicating deficient coupling to G $\alpha_i$  and lack of effect on G $\alpha_s$ -stimulation. Hence the R148K mutant may prevent mobilization of G $\beta\gamma$ , perhaps by binding free G $\beta\gamma$  subunits. Other mutants appeared to convert DPAT agonism to inverse or biased agonism, as suggested by DPAT-induced potentiation of

dopamine-D1 receptor stimulation (Fig. 1B). For these mutants and wild-type 5-HT1A receptors, DPAT had no detectable effect on basal cAMP levels. Thus co-activation of Gs by D1 receptor activation was required to observe DPAT-induced potentiation. This enhancement of D1 response was blocked by pertussis toxin treatment indicating that the potentiation is mediated by Gi/Go proteins and is not due to weak agonist-mediated stimulation of Gs as observed for mutants of 5-HT1A Ci3 domain (Malmberg and Strange, 2000). DPAT-induced potentiation was greatest for the P150T-5-HT1A receptor, which lacked coupling to adenylyl cyclase II. Oppositely the R148K mutant that inhibited adenylyl cyclase II had no effect on D1-stimulated cAMP. Thus, distinct mutations of the Ci2 domain of the 5-HT1A receptor reduced basal activity or altered agonist function.

*Functional 5-HT1A mutants:* Mutations at the T149 and Y144 sites, the most conserved residues in the Ci2 domain (Albert et al., 1998), resulted in receptors that retained the most complete coupling. The T149 mutants all coupled to G $\alpha$ i and several retained G $\beta$  $\gamma$  coupling, indicating that the polar hydroxyl residue of T149 is dispensable for coupling (Table I, Fig. 2). The T149G mutant coupled better to phospholipase C while T149R coupled better to adenylyl cyclase II, indicating that G $\beta$  $\gamma$  effector selectivity was affected by mutations at this site. The negatively-charged T149E mutant, which mimics phospho-threonine, displayed weak G $\beta$  $\gamma$  coupling, but normal G $\alpha$ i coupling. Similarly, activation of protein kinase C, which phosphorylates the 5-HT1A receptor (Raymond, 1991) at several sites, including T149 (Kushwaha and Albert, unpublished), selectively uncouples G $\beta$  $\gamma$  signaling, with little effect on G $\alpha$ i signaling (Kushwaha and Albert, 2005; Lembo and Albert, 1995; Wu et al., 2002). The results from T149 mutants displayed selective impairments of G $\beta$  $\gamma$  signaling indicating that the T149 site is critical for

selective coupling of G $\beta\gamma$  subunits. Mutational analysis of the Y144 residue revealed that this is the most important Ci2 site in directing coupling of 5-HT1A receptors to both G $\alpha_i$  and G $\beta\gamma$  signaling. For example, the conservative Y144F mutation retained coupling to G $\beta\gamma$ /adenylyl cyclase II and G $\alpha_i$ , but not to G $\beta\gamma$ /phospholipase C, indicating a key role for the polar hydroxyl moiety of Y144 in coupling. The Y144A mutant coupled effectively to G $\beta\gamma$ /adenylyl cyclase II, but not to G $\alpha_i$  or G $\beta\gamma$ /phospholipase C, while the Y144N mutant coupled to G $\alpha_i$  and G $\beta\gamma$ /phospholipase C, but not to G $\beta\gamma$ /adenylyl cyclase II. This diversity of Y144 mutant signaling phenotypes indicates a critical role for the Y144 residue as a signaling terminus that is critical for the specificity of receptor coupling to G $\alpha_i$  and G $\beta\gamma$ .



## DISCUSSION

Structure-function studies of GPCR coupling to G-proteins have implicated the receptor i2 and i3 loops in G-protein activation, particularly the highly-conserved N-terminal E/DRY i2 motif (Wess et al., 1997; Shapiro et al, 2002), but the role of the Ci2 domain is undetermined. Previous studies have examined primarily G $\alpha$ -mediated signaling, but the structural determinants of G $\beta\gamma$ -mediated signaling remain to be addressed (Bourne, 1997). Given that specific receptor- and effector-dependent G $\beta\gamma$  combinations mediate G $\beta\gamma$  signaling, accumulating data suggest that direct receptor-G $\beta\gamma$  interactions may underlie this specificity (Albert and Robillard, 2002; Chidiac, 1998; Clapham and Neer, 1997). We have examined the coupling of point mutants at each residue of the 5-HT1A Ci2 domain to G $\alpha$ i- or G $\beta\gamma$ -mediated pathways. The majority of 5-HT1A-Ci2 mutant receptors displayed ligand binding that was comparable to wild type receptors. However most point mutants were uncoupled, either selectively from G $\beta\gamma$  or from both G $\beta\gamma$  and G $\alpha$ I signaling. This represents the first detailed evidence that the entire Ci2 domain plays a key role in receptor signaling to both G $\beta\gamma$  and G $\alpha$ , which was unexpected given its limited primary sequence homology of this domain (Albert et al., 1998). The sequence divergence of Ci2 domains may determine receptor-dependent G $\beta\gamma$  specificity.

Although mutations in the Ci2 domain did not affect the predicted amphipathic  $\alpha$ -helical secondary structure, mutations that altered the predicted coil localized at P150 resulted in completely uncoupled or inversely-coupled receptors (Supplemental Table 2). The ACII assay provides a sensitive measure of ligand-independent 5-HT1A receptor activity that is sensitive to PTX, and G $\beta\gamma$  scavengers, allowing determination constitutive activity (Albert et al., 1999). Two mutants displayed inverse basal activity towards ACII (R148K, P150D) while other mutants switched coupling of the full agonist DPAT to inverse agonism (Fig. 1B). Notably,

substitutions at P150 generated receptors with inverse agonist properties at  $G_{\alpha i}$  or inverse basal coupling to  $G\beta\gamma$  responses. The loss of the coil induced by mutations at P150 may transmit a general perturbation to completely inhibit weak basal activity the receptor.

In order to visualize the potential roles of the Ci2 domain residues in tertiary receptor structure, a computer model of the 5-HT1A receptor based on the X-ray crystal structure of bovine rhodopsin (Palczewski et al., 2000) was generated (Fig. 3). This model predicts that the Ci2 domain lies in close proximity to the Ni2, Ni3 and Ci3 portions of intracellular loops. In particular, the model predicts that Ci2 residues Y144 and K147 lie in close proximity to Ci3 residue E340, possibly forming hydrogen, van der Waals or ionic bonds. Viewed from a rotated angle (Fig. 3C), it becomes apparent that K147 and R148 are in close proximity to D133 and could interact with the conserved DRY motif—perhaps via ionic or other types of interactions. The R134 site is also predicted to be near enough to E340 (Ci3) to facilitate intramolecular interactions between Ni2 (DRY motif), Ci2 (YXXKR motif) and Ci3 (E340). A similar network of interactions between i2 and Ci3 via the DRY motif and the homologous E318 residue of the 5-HT2A receptor has been noted previously (Shapiro et al., 2002). The lack of coupling of the K147R- and R148K-5-HT1A receptors suggests that the  $\epsilon$ -amino or guanidinium side-chains of these residues make specific, spatially restricted interactions. Mutations of Y144 showed the greatest diversity of coupling phenotypes (depending on the substitution), suggesting that this site not only stabilizes receptor coupling domains, but could also have direct interactions with  $G\beta\gamma$  subunits to determine signaling selectivity. The YXXKR motif is absolutely conserved in all 5-HT1A receptor homologues (to *C. elegans*), as well as in several 5-HT1, muscarinic (M1-5), and adrenergic ( $\alpha 2$ ) receptors and the Y144 residue is highly conserved among Class I GPCRs (Albert et al., 1998), suggesting a conserved role in these receptors. Our data support the

importance of the YXXKR residues in determining the efficiency and selectivity 5-HT1A receptor coupling.

Our previous studies had implicated T149 in G $\beta\gamma$  coupling of the 5-HT1A receptor (Albert et al., 1999; Kushwaha and Albert, 2005; Lembo et al., 1997; Wu et al., 2002) and Thr149 mutants all retained coupling to G $\alpha_i$ , but were selectively uncoupled from G $\beta\gamma$ . For example, the T149G mutant coupled better to PLC $\beta$ -mediated calcium mobilization than to stimulation of ACII, whereas the T149R mutant coupled better to ACII than to PLC $\beta$ . The polar hydroxyl group of Thr149 is predicted to project outward from hydrophilic face of the receptor (Fig. 3C) and could stabilize G $\beta\gamma$  binding to the receptor. Similarly, N146 and D143 mutations also retained coupling to G $\alpha_i$  but had selective impairments in G $\beta\gamma$  signaling. Like Thr149, the side-chains of these residues are polar and are also predicted to project outwards into the cytoplasmic face (Fig. 3B, C) and may stabilize G $\beta\gamma$  interactions. In summary our data are consistent with a model of positively charged residues in the 5-HT1A-Ci2 domain that create a hydrophilic face that permits specific interactions of polar side-chains of D143, N146 and T149 to mediate G $\beta\gamma$  coupling.

In contrast to the 5-HT1A Ci2 domain, the i3 loop (Ni3 and Ci3) has been implicated in G-protein signaling, but mainly to coupling to G $\alpha_i$ . Peptides corresponding to the 5-HT1A Ci3 domain mimic G $\alpha_i$ -mediated inhibition of forskolin-stimulated AC and attenuate inhibitory coupling of 5-HT1A receptors to AC (Malmberg and Strange, 2000; Ortiz et al., 2000). Similarly, 5-HT1A-i2 loop peptides mediate direct coupling to inhibition of cAMP (Varrault et al., 1994) Mutation of Ci3 residues (V344E and T343A/V344E) enhanced receptor coupling to G $s$  over G $i$ , consistent with its role in determining G $\alpha_i$  specificity (Malmberg and Strange, 2000). Thus, while Ci3 appears to mainly dictate G $\alpha_i$  specificity, our results indicate that Ci2 is

mainly implicated in  $G\beta\gamma$  signaling but also contributes to  $G\alpha_i$  signaling. The C-terminal domain of the 5-HT<sub>1A</sub> receptor also appears to be critical for coupling to both  $G\alpha_i$  and  $G\beta\gamma$  pathways. Unlike other receptors, the 5-HT<sub>1A</sub> receptor is constitutively palmitoylated at C-terminal cysteine residues (417 and 420) and palmitoylation is required for coupling to  $G_i$  (i.e. loss of inhibition of AC activity) and  $G\beta\gamma$ -mediated activation of ERKs (Papoucheva et al., 2004). Thus, Ci<sub>2</sub>, Ni<sub>3</sub>, Ci<sub>3</sub> and palmitoylated 5-HT<sub>1A</sub> C-terminal domains appear critical for G-protein coupling, and may directly interact to form a G-protein coupling interface.

In summary, our mutagenesis studies show that multiple residues in the Ci<sub>2</sub> sequence <sup>143</sup>DYVNRTPRR<sup>152</sup> are implicated in 5-HT<sub>1A</sub> receptor coupling to  $G\beta\gamma$  and  $G\alpha_i$ . The pattern of mutations predicts that the positively-charged face of the predicted amphipathic Ci<sub>2</sub> alpha-helix is absolutely required for coupling and that uncharged residues in this face (T149, N146) direct  $G\beta\gamma$  but not  $G\alpha_i$  coupling. The opposite inwardly-oriented face includes a critical Y144 residue that directs the specificity of coupling to both  $G\beta\gamma$  and  $G\alpha_i$  pathways, and interacts with the Ci<sub>3</sub> or Ni<sub>2</sub> loops forming the G-protein coupling interface.

REFERENCES:

- Albert PR and Lemonde S (2004) 5-HT1A Receptors, Gene Repression, and Depression: Guilt by Association. *Neuroscientist* **10**:575-93.
- Albert PR, Morris SJ, Ghahremani MH, Storrington JM and Lembo PM (1998) A putative alpha-helical G beta gamma-coupling domain in the second intracellular loop of the 5-HT1A receptor. *Ann N Y Acad Sci* **861**:146-61.
- Albert PR and Robillard L (2002) G protein specificity. Traffic direction required. *Cell Signal* **14**:407-18.
- Albert PR, Sajedi N, Lemonde S and Ghahremani MH (1999) Constitutive G(i2)-dependent activation of adenylyl cyclase type II by the 5-HT1A receptor. Inhibition by anxiolytic partial agonists. *J Biol Chem* **274**:35469-74.
- Ballesteros JA, Jensen AD, Liapakis G, Rasmussen SG, Shi L, Gether U and Javitch JA (2001) Activation of the beta 2-adrenergic receptor involves disruption of an ionic lock between the cytoplasmic ends of transmembrane segments 3 and 6. *J Biol Chem* **276**:29171-7.
- Bourne HR (1997) How receptors talk to trimeric G proteins. *Curr Opin Cell Biol* **9**:134-42.
- Burstein ES, Spalding TA and Brann MR (1996) Amino acid side chains that define muscarinic receptor/G-protein coupling. Studies of the third intracellular loop. *J Biol Chem* **271**:2882-5.
- Burstein ES, Spalding TA and Brann MR (1998) The second intracellular loop of the m5 muscarinic receptor is the switch which enables G-protein coupling. *J Biol Chem* **273**:24322-7.
- Chidiac P (1998) Rethinking receptor-G protein-effector interactions. *Biochem Pharmacol* **55**:549-56.

Clapham DE and Neer EJ (1997) G protein beta gamma subunits. *Ann Rev Pharmacol & Toxicol* **37**:167-203.

Gross C and Hen R (2004) The developmental origins of anxiety. *Nat Rev Neurosci* **5**:545-52.

Hill-Eubanks D, Burstein ES, Spalding TA, Brauner-Osborne H and Brann MR (1996) Structure of a G-protein-coupling domain of a muscarinic receptor predicted by random saturation mutagenesis. *J Biol Chem* **271**:3058-65.

Kushwaha N and Albert PR (2005) Coupling of 5-HT<sub>1A</sub> autoreceptors to inhibition of mitogen-activated protein kinase activation via Gbetagamma subunit signaling. *Eur J Neurosci* **21**:721-32.

Lembo PM and Albert PR (1995) Multiple phosphorylation sites are required for pathway-selective uncoupling of the 5-hydroxytryptamine<sub>1A</sub> receptor by protein kinase C. *Mol Pharmacol* **48**:1024-9.

Lembo PM, Ghahremani MH, Morris SJ and Albert PR (1997) A conserved threonine residue in the second intracellular loop of the 5- hydroxytryptamine <sub>1A</sub> receptor directs signaling specificity. *Mol Pharmacol* **52**:164-71.

Liu J, Conklin BR, Blin N, Yun J and Wess J (1995) Identification of a receptor/G-protein contact site critical for signaling specificity and G-protein activation. *Proc Natl Acad Sci U S A* **92**:11642-6.

Liu YF and Albert PR (1991) Cell-specific signaling of the 5-HT<sub>1A</sub> receptor. Modulation by protein kinases C and A. *J Biol Chem* **266**:23689-97.

Liu YF, Ghahremani MH, Rasenick MM, Jakobs KH and Albert PR (1999) Stimulation of cAMP Synthesis by Gi-coupled receptors upon ablation of distinct Galphai protein expression. Gi subtype specificity of the 5-HT<sub>1A</sub> receptor. *J Biol Chem* **274**:16444-16450.

- Malmberg A and Strange PG (2000) Site-directed mutations in the third intracellular loop of the serotonin 5-HT(1A) receptor alter G protein coupling from G(i) to G(s) in a ligand-dependent manner. *J Neurochem* **75**:1283-93.
- Meng EC and Bourne HR (2001) Receptor activation: what does the rhodopsin structure tell us? *Trends Pharmacol Sci* **22**:587-93.
- Ortiz TC, Devereaux MC, Jr. and Parker KK (2000) Structural variants of a human 5-HT1a receptor intracellular loop 3 peptide. *Pharmacology* **60**:195-202.
- Palczewski K, Kumasaka T, Hori T, Behnke CA, Motoshima H, Fox BA, Le Trong I, Teller DC, Okada T, Stenkamp RE, Yamamoto M and Miyano M (2000) Crystal structure of rhodopsin: A G protein-coupled receptor. *Science* **289**:739-45.
- Papoucheva E, Dumuis A, Sebben M, Richter DW and Ponimaskin EG (2004) The 5-hydroxytryptamine(1A) receptor is stably palmitoylated, and acylation is critical for communication of receptor with Gi protein. *J Biol Chem* **279**:3280-91.
- Pineyro G and Blier P (1999) Autoregulation of serotonin neurons: role in antidepressant drug action. *Pharmacol Rev* **51**:533-91.
- Raymond JR (1991) Protein kinase C induces phosphorylation and desensitization of the human 5-HT1A receptor. *J Biol Chem* **266**:14747-53.
- Sakmar TP, Menon ST, Marin EP and Awad ES (2002) Rhodopsin: insights from recent structural studies. *Annu Rev Biophys Biomol Struct* **31**:443-84.
- Schmidt C, Li B, Bloodworth L, Erlenbach I, Zeng FY and Wess J (2003) Random mutagenesis of the M3 muscarinic acetylcholine receptor expressed in yeast. Identification of point mutations that "silence" a constitutively active mutant M3 receptor and greatly impair receptor/G protein coupling. *J Biol Chem* **278**:30248-60.

- Setola V, Dukat M, Glennon RA and Roth BL (2005) Molecular determinants for the interaction of the valvulopathic anorexigen norfenfluramine with the 5-HT<sub>2B</sub> receptor. *Mol Pharmacol* **68**:20-33.
- Shapiro DA, Kristiansen K, Weiner DM, Kroeze WK and Roth BL (2002) Evidence for a model of agonist-induced activation of 5-hydroxytryptamine 2A serotonin receptors that involves the disruption of a strong ionic interaction between helices 3 and 6. *J Biol Chem* **277**:11441-11449.
- Shi L, Liapakis G, Xu R, Guarnieri F, Ballesteros JA and Javitch JA (2002) Beta2 adrenergic receptor activation. Modulation of the proline kink in transmembrane 6 by a rotamer toggle switch. *J Biol Chem* **277**:40989-96.
- Spalding TA, Burstein ES, Henderson SC, Ducote KR and Brann MR (1998) Identification of a ligand-dependent switch within a muscarinic receptor. *J Biol Chem* **273**:21563-8.
- Sun QQ and Dale N (1999) G-proteins are involved in 5-HT receptor-mediated modulation of N- and P/Q- but not T-type Ca<sup>2+</sup> channels. *J Neurosci* **19**:890-9.
- Thiagaraj HV, Ortiz TC, Burnett A and Parker KK (2002) G protein coupling and activation characteristics of intracellular loops 2 and 3 of the 5-HT<sub>1A</sub> receptor. *Trends Compar Biochem Physiol* **9**:117-129.
- Turner JH, Gelasco AK and Raymond JR (2004) Calmodulin interacts with the third intracellular loop of the serotonin 5-hydroxytryptamine<sub>1A</sub> receptor at two distinct sites: putative role in receptor phosphorylation by protein kinase C. *J Biol Chem* **279**:17027-37.
- Varrault A, Le Nguyen D, McClue S, Harris B, Jouin P and Bockaert J (1994) 5-Hydroxytryptamine<sub>1A</sub> receptor synthetic peptides. Mechanisms of adenylyl cyclase inhibition. *J Biol Chem* **269**:16720-5.



- Wess J, Liu J, Blin N, Yun J, Lerche C and Kostenis E (1997) Structural basis of receptor/G protein coupling selectivity studied with muscarinic receptors as model systems. *Life Sci* **60**:1007-14.
- Wu X, Kushwaha N, Albert PR and Penington NJ (2002) A critical protein kinase C phosphorylation site on the 5-HT(1A) receptor controlling coupling to N-type calcium channels. *J Physiol* **538**:41-51.
- Wurch T, Colpaert FC and Pauwels PJ (2003) Mutation in a protein kinase C phosphorylation site of the 5-HT(1A) receptor preferentially attenuates Ca(2+) responses to partial as opposed to higher-efficacy 5-HT(1A) agonists. *Neuropharmacology* **44**:873-81.
- Zeng FY, Hopp A, Soldner A and Wess J (1999) Use of a disulfide cross-linking strategy to study muscarinic receptor structure and mechanisms of activation. *J Biol Chem* **274**:16629-40.

## **FOOTNOTES**

<sup>#</sup>Department of Psychiatry, Center for Neurobiology and Psychiatry, Institute for Neurodegenerative Diseases, University of California, San Francisco School of Medicine, San Francisco, CA 94143.

<sup>##</sup>Department of Psychiatry, Case Western Reserve University Medical School, Cleveland, OH 44106.

\*Corresponding author.

<sup>1</sup>This work was supported by a grant from the Canadian Institutes of Health Research (CIHR) to P.R.A. and a CIHR Doctoral Award to N.K. P.R.A. is the CIHR/Novartis Michael Smith Chair in Neuroscience. M.B. was supported by a National Institute of Mental Health National Research Service Award (F31 MH075708-01) and the Medical Scientist Training Program at UCSF. L.H.T. was supported by the National Institutes of Health (NIH) and B.L.R. was supported by NIH grants MH57635 and KO2MH01366.

## FIGURE LEGENDS

### **FIG. 1. Inverse agonist function of 5-HT1A-i2 mutant receptors on G $\alpha$ i and G $\beta$ $\gamma$ responses.**

*A*, Agonist independent G $\beta$  $\gamma$ -mediated activation of adenylyl cyclase II. HEK 293 cells were transiently transfected with expression plasmids for adenylyl cyclase II, G $\alpha$ i2, and the indicated wild type (1A) or i2 mutant 5-HT1A receptors and agonist-independent cAMP production was measured. Constitutive receptor activity was determined using the average difference between pertussis toxin-treated and non-treated cells, normalized to wild type 5-HT1A activity (100%) for 3-6 independent experiments. Significant difference of receptor activity from zero (pertussis toxin-treated) was calculated using paired t-test, \*\* $p < 0.01$ , \* $p < 0.05$ . *B*, Agonist-induced inhibition of Gs-stimulated cAMP accumulation. HEK 293 cells were transiently co-transfected with expression plasmids for dopamine-D1 receptor and wild type or mutant 5-HT1A receptor. Cells were treated with dopamine agonist apomorphine (10  $\mu$ M) (control) or apomorphine and 5-HT1A agonist 8-OH-DPAT (1  $\mu$ M) and cAMP was measured. Values were normalized to apomorphine-stimulated cAMP accumulation (100%). Significant differences from 100% were calculated using paired t-test, \*\* $p < 0.01$ , \* $p < 0.05$ .

### **FIG 2. Coupling of 5-HT1A-i2 mutants to calcium mobilization is Gi/Go-specific.**

Fibroblast Ltk- cells were transiently transfected with either 5  $\mu$ g of wild type 5-HT1A (1A) or 5-HT1A-i2 T149 mutant receptors (i2 (T149A), Gly (T149G), Arg (T149R)), and changes in intracellular free calcium concentration in response to 5-HT1A agonist DPAT (1  $\mu$ M; solid line) were measured (*see Experimental Methods*). Calcium mobilization of the wild type (1A) and mutant 5-HT1A receptors was blocked by pre-treatment with pertussis toxin (50 ng/ml, 16h;

dashed line). Response to ATP (10  $\mu$ M; solid line) was used as a positive control. Traces shown are representative; similar results were obtained from at least three independent experiments.

**FIG. 3. Predicted structural model of the wild type rat 5-HT<sub>1A</sub> receptor.**

The depicted model of the rat 5-HT<sub>1A</sub> receptor was based on the high resolution crystal structure of bovine rhodopsin in its inactive state and homology with previously published 5-HT receptor models (Shapiro et al, 2002; Setola et al, 2005; see METHODS) and visualized using Protein Explorer (PE, [http:// www.proteinexplorer.org](http://www.proteinexplorer.org)). *A*, Side view of the wild type 5-HT<sub>1A</sub> receptor. The  $\alpha$ -helices are shown in pink,  $\beta$ -sheets are labeled with orange arrows, and the i2 and i3 loops are indicated. *B*, Amino acids of the N- and C-terminal regions of the i2 and i3 loops (Ni2, Ni3, Ci2, and Ci3) are indicated. Potential predicted inter-helical ionic and/or hydrogen bonding between side-chains of Ci3 residue Glu340 (E340) and Ci2 residues Tyr144/Lys147 (Y144/K147) are indicated by a dashed green line. *C*, Detailed view of the i2 loop domain showing predicted secondary structure, alpha-helices are colored *pink* and beta-sheets are in *gray*. Predicted coordinate hydrogen and ionic bonding of Tyr144/Lys147 (Ci2), Asp133/Arg134 (Ni2 DRY motif) and Glu340 (Ci3) are indicated as a green dashed line.

**TABLE I. Summary of binding, G $\alpha$ i- and G $\beta$  $\gamma$ -coupling properties of 5-HT1A-i2 mutants.**

Agonist-induced changes in intracellular free calcium concentration in Ltk- cells transiently transfected with wild type 5-HT1A (1A) or 5-HT1A-i2 mutant receptors were measured and quantified as percent control over basal  $[Ca^{2+}]_i$  levels (*Column 1*), \*NR: no response to treatments. In parallel experiments, membranes were prepared from Ltk- cells transiently transfected with the indicated 5-HT1A mutant receptors and subjected to binding analysis with  $[^3H]$ -OH-DPAT (*Column 2*). Agonist independent G $\beta$  $\gamma$ -mediated activation of adenylyl cyclase II was determined using HEK 293 cells transiently transfected with expression plasmids for adenylyl cyclase II, G $\alpha$ i2, and the indicated wild type (1A) or i2 mutant 5-HT1A receptor. Agonist-independent cAMP production was determined using the average difference between pertussis toxin-treated and non-treated cells for 3-6 independent experiments, where (+++) indicates  $\geq 80\%$ , (++)  $\geq 50\%$ , and (+) between 19-27% increase in cAMP production compared to wild-type 5-HT1A receptor and (-), no detectable activity (*Column 3*). For G $\alpha$ i-mediated inhibition of adenylyl cyclase, HEK cells were transiently co-transfected with 12  $\mu$ g of D1 receptor cDNA and an equal amount of wild type (1A) or 5-HT1A-i2 mutant receptors. Inhibition of D1/G $\alpha$ s-stimulated (10  $\mu$ M Apomorphine) cAMP accumulation by 5-HT1A agonist 8-OH-DPAT (1  $\mu$ M) was measured by specific RIA and data were presented as percent inhibition of D1-stimulated cAMP levels (*Column 4*). In all cases, data are expressed as mean  $\pm$  SEM of at least three independent experiments, and values that are significantly different from zero were identified using Student's paired t-test and are indicated, \*\*\*p <0.001, \*\*p<0.01, \*p<0.05.

| SUBSTITUTION | DPAT-INDUCED $\uparrow$ $[Ca^{2+}]_i$ (% over basal $[Ca^{2+}]_i$ ) | RECEPTOR NUMBER (pmol/transfection) | CONSTITUTIVE ACTIVITY (Level of coupling to $\beta\gamma$ -mediated stimulation of ACII) | % INHIBITION OF D1-STIMULATED cAMP ACCUMULATION |
|--------------|---|-------------------------------------|--|---|
| WT (1A)      | 101 $\pm$ 8 <sup>**</sup>   | 1.9 $\pm$ 0.4 <sup>*</sup>          | +++  | 48 $\pm$ 9 <sup>*</sup>                         |
| T149A (i2)   | 27 $\pm$ 9 <sup>*</sup>   | 2.3 $\pm$ 0.7 <sup>*</sup>          | +  | 53 $\pm$ 10 <sup>*</sup>                        |
| D143F        | 15 $\pm$ 3 <sup>*</sup>   | 1.5 $\pm$ 0.9                       | -  | 54 $\pm$ 8 <sup>**</sup>                        |
| D143V        | 22 $\pm$ 4 <sup>*</sup>   | 2.5 $\pm$ 0.2 <sup>**</sup>         | -  | 56 $\pm$ 9 <sup>**</sup>                        |
| D143N        | 26 $\pm$ 7 <sup>*</sup>   | 0.9 $\pm$ 0.1 <sup>**</sup>         | -  | 45 $\pm$ 9 <sup>*</sup>                         |
| D143L        | 29 $\pm$ 7 <sup>*</sup>   | 0.7 $\pm$ 0.4                       | -  | 52 $\pm$ 3 <sup>**</sup>                        |
| D143C        | NR  | 2.9 $\pm$ 0.8 <sup>*</sup>          | -  | 44 $\pm$ 12 <sup>*</sup>                        |
| Y144H        | NR  | 1.9 $\pm$ 0.2 <sup>**</sup>         | -  | 22 $\pm$ 3 <sup>**</sup>                        |
| Y144A        | 4 $\pm$ 2   | 1.7 $\pm$ 0.5 <sup>*</sup>          | +++  | 11 $\pm$ 8                                      |
| Y144N        | 25 $\pm$ 7 <sup>*</sup>   | 2.4 $\pm$ 0.6 <sup>*</sup>          | -  | 44 $\pm$ 5 <sup>**</sup>                        |
| Y144F        | NR  | 2.3 $\pm$ 0.6 <sup>*</sup>          | ++   | 43 $\pm$ 7 <sup>**</sup>                        |
| Y144V        | 10 $\pm$ 6  | 2.3 $\pm$ 0.2 <sup>**</sup>         | -  | 7 $\pm$ 2 <sup>*</sup>                          |
| Y144I        | NR  | 1.4 $\pm$ 0.7                       | -  | 26 $\pm$ 5 <sup>*</sup>                         |
| Y144C        | NR  | 2.1 $\pm$ 1.1                       | -  | -20 $\pm$ 3 <sup>**</sup>                       |
| V145L        | 26 $\pm$ 3 <sup>**</sup>  | 2.2 $\pm$ 0.9                       | +  | 34 $\pm$ 11 <sup>*</sup>                        |
| V145K        | 23 $\pm$ 9 <sup>*</sup>   | 1.4 $\pm$ 0.2 <sup>**</sup>         | +  | 41 $\pm$ 13 <sup>*</sup>                        |
| V145Y        | 4 $\pm$ 3   | 1.3 $\pm$ 0.7                       | -  | -30 $\pm$ 10 <sup>*</sup>                       |
| V145R        | NR  | 1.6 $\pm$ 0.6 <sup>*</sup>          | -  | 15 $\pm$ 9                                      |
| V145Q        | NR  | 1.9 $\pm$ 0.2 <sup>**</sup>         | -  | 27 $\pm$ 7 <sup>*</sup>                         |
| V145E        | 12 $\pm$ 5  | 1.8 $\pm$ 0.5 <sup>*</sup>          | -  | 32 $\pm$ 9 <sup>*</sup>                         |
| V145S        | NR  | 1.5 $\pm$ 0.6 <sup>*</sup>          | -  | -12 $\pm$ 7                                     |
| V145W        | NR  | 1.2 $\pm$ 0.2 <sup>**</sup>         | -  | 17 $\pm$ 6 <sup>*</sup>                         |
| N146T        | 56 $\pm$ 17 <sup>*</sup>  | 1.8 $\pm$ 0.3 <sup>**</sup>         | ++   | 31 $\pm$ 8 <sup>*</sup>                         |
| N146F        | 14 $\pm$ 5 <sup>*</sup>   | 1.9 $\pm$ 0.7 <sup>*</sup>          | -  | 42 $\pm$ 10 <sup>*</sup>                        |
| N146A        | 20 $\pm$ 13   | 1.0 $\pm$ 0.2 <sup>*</sup>          | -  | 53 $\pm$ 10 <sup>*</sup>                        |
| K147R        | NR  | 2.3 $\pm$ 0.6 <sup>*</sup>          | -  | -3 $\pm$ 6                                      |
| K147Q        | NR  | 2.5 $\pm$ 1.2                       | -  | -11 $\pm$ 9                                     |
| R148L        | 17 $\pm$ 5 <sup>*</sup>   | 2.5 $\pm$ 0.4 <sup>**</sup>         | -  | 13 $\pm$ 4 <sup>*</sup>                         |
| R148Q        | 16 $\pm$ 2 <sup>**</sup>  | 1.3 $\pm$ 0.2 <sup>**</sup>         | -  | 20 $\pm$ 8 <sup>*</sup>                         |
| R148K        | 12 $\pm$ 6  | 2.1 $\pm$ 0.1 <sup>***</sup>        | -  | 4 $\pm$ 10                                      |
| R148E        | 28 $\pm$ 4 <sup>**</sup>  | 1.5 $\pm$ 0.1 <sup>**</sup>         | -  | 20 $\pm$ 3 <sup>**</sup>                        |

|              |                 |                     |     |                  |
|--------------|-----------------|---------------------|-----|------------------|
| <b>R148P</b> | NR              | $3.2 \pm 0.9^*$     | +   | $21 \pm 4^{**}$  |
| <b>R148G</b> | $19 \pm 6^*$    | $2.8 \pm 1.1^*$     | +   | $53 \pm 10^*$    |
| <b>R148V</b> | $20 \pm 9$      | $1.2 \pm 0.4^*$     | -   | $45 \pm 8^*$     |
| <b>T149E</b> | $20 \pm 4^*$    | $1.0 \pm 0.4^*$     | +   | $50 \pm 3^{**}$  |
| <b>T149V</b> | $10 \pm 5$      | $1.7 \pm 1.0$       | -   | $46 \pm 14^*$    |
| <b>T149G</b> | $80 \pm 8^{**}$ | $3.3 \pm 0.6^*$     | ++  | $52 \pm 8^{**}$  |
| <b>T149R</b> | $50 \pm 3^{**}$ | $1.5 \pm 0.9$       | +++ | $60 \pm 8^{**}$  |
| <b>T149Q</b> | $22 \pm 2^{**}$ | $1.8 \pm 0.8$       | +   | $39 \pm 4^{**}$  |
| <b>T149M</b> | $15 \pm 7$      | $1.9 \pm 0.2^{**}$  | -   | $42 \pm 4^{**}$  |
| <b>T149W</b> | $9 \pm 7$       | $2.0 \pm 0.7^*$     | -   | $44 \pm 5^{**}$  |
| <b>T149P</b> | $6 \pm 9$       | $2.6 \pm 0.4^{**}$  | ++  | $27 \pm 9^*$     |
| <b>P150R</b> | $2 \pm 5$       | $2.3 \pm 0.1^{***}$ | -   | $-6 \pm 3$       |
| <b>P150N</b> | NR              | $1.3 \pm 0.8$       | -   | $-12 \pm 1^{**}$ |
| <b>P150D</b> | NR              | $1.3 \pm 0.2^{**}$  | -   | $4 \pm 2$        |
| <b>P150G</b> | NR              | $2.0 \pm 1.0$       | -   | $-6 \pm 1^{**}$  |
| <b>P150I</b> | $7 \pm 8$       | $1.7 \pm 0.2^{**}$  | -   | $4 \pm 1^*$      |
| <b>P150L</b> | NR              | $0.9 \pm 0.6$       | -   | $-23 \pm 9^*$    |
| <b>P150F</b> | NR              | $1.9 \pm 0.5^*$     | -   | $15 \pm 11$      |
| <b>P150S</b> | NR              | $0.8 \pm 0.1^{**}$  | -   | $-19 \pm 10$     |
| <b>P150T</b> | NR              | $2.1 \pm 0.8^*$     | -   | $-48 \pm 9^*$    |
| <b>R151Q</b> | $4 \pm 6$       | $1.7 \pm 0.8$       | -   | $22 \pm 8^*$     |
| <b>R151A</b> | $26 \pm 4^{**}$ | $2.3 \pm 0.9^*$     | +   | $24 \pm 8^*$     |
| <b>R151M</b> | $8 \pm 1^{**}$  | $2.1 \pm 1.0$       | -   | $20 \pm 4^*$     |
| <b>R151T</b> | $27 \pm 3^{**}$ | $1.0 \pm 0.1^{**}$  | +   | $38 \pm 7^*$     |
| <b>R151L</b> | $2 \pm 5$       | $0.8 \pm 0.2^*$     | -   | $30 \pm 6^*$     |
| <b>R151K</b> | $2 \pm 4$       | $1.5 \pm 1.1$       | -   | $26 \pm 6^*$     |
| <b>R152N</b> | $16 \pm 4^*$    | $1.4 \pm 0.6$       | -   | $10 \pm 7$       |
| <b>R152V</b> | $8 \pm 7$       | $1.3 \pm 0.5^*$     | -   | $37 \pm 8^*$     |
| <b>R152A</b> | $13 \pm 7$      | $2.2 \pm 0.9^*$     | -   | $56 \pm 7^{**}$  |
| <b>R152P</b> | $26 \pm 3^{**}$ | $1.1 \pm 0.5$       | -   | $12 \pm 11$      |
| <b>R152D</b> | $27 \pm 6^*$    | $1.5 \pm 0.8$       | -   | $-11 \pm 2$      |

**TABLE II. Signaling phenotypes of mutant 5-HT1A receptors.**

Mutant 5-HT1A receptors were grouped according to their responses in the  $G\alpha_i$ -mediated (% inhibition of DA-stimulated cAMP accumulation) and  $G\beta\gamma$ -mediated (DPAT-induced increase in intracellular calcium, and  $G\beta\gamma$ -mediated stimulation of adenylyl cyclase II) assays. For  $G\beta\gamma$  assays the maximal response produced by wild-type 5-HT1A receptor was designated as 100%. Wild type-like receptors, include mutants with adenylyl cyclase II coupling of  $\geq 50\%$  and calcium mobilization  $\geq 60\%$  of wild-type 5-HT1A receptor, and inhibition of cAMP accumulation  $\geq 30\%$ .  $G\alpha_i$ -coupled/weak  $G\beta\gamma$ -coupled mutants, include receptors that behave like the 5-HT1A-T149A receptor. These mutants had adenylyl cyclase II coupling of  $\leq 30\%$  and calcium mobilization 19-27% of wild-type 5-HT1A receptor, and inhibition of cAMP accumulation 24-53%. Uncoupled mutants had undetectable responses.  $G\beta\gamma$ -uncoupled mutants include receptors that were uncoupled from both  $G\beta\gamma$  responses (calcium mobilization and adenylyl cyclase II), but still retained  $G\alpha_i$  function (inhibition of cAMP).  $G\beta\gamma$ -selective coupled, include receptors that possess at least one intact  $G\beta\gamma$  response. Receptors have been separated into two categories: i) mutants that couple to adenylyl cyclase II stimulation and ii) mutants that couple to phospholipase  $C\beta$ -mediated calcium mobilization. Several receptor mutants also displayed inverse activity. Some mutants inhibited the basal activity of adenylyl cyclase II, and others potentiated DPAT-induced D1 receptor stimulation to increase cAMP accumulation.



| Ci2 Residue | Wild-type-like | G $\alpha$ i-coupled/<br>weak G $\beta$ $\gamma$ -coupled | Uncoupled   | G $\beta$ $\gamma$ -uncoupled    | G $\beta$ $\gamma$ -selective coupled |                                  | Inverse basal activity |                                   |
|-------------|----------------|---|---|----------------------------------|---------------------------------------|----------------------------------|------------------------|-----------------------------------|
|             |                |   |   |                                  | ACII                                  | PLC $\beta$                      | ACII                   | Potential of DA-stimulated [cAMP] |
| <b>D143</b> |                |   |   | D143C                            |                                       | D143F<br>D143V<br>D143N<br>D143L |                        |                                   |
| <b>Y144</b> |                |   | Y144V<br>Y144C  | Y144H<br>Y144I                   | Y144A<br>Y144F                        | Y144N                            |                        | Y144C                             |
| <b>V145</b> |                | V145L<br>V145K  | V145R<br>V145S  | V145Q<br>V145E<br>V145W          |                                       |                                  |                        | V145Y                             |
| <b>N146</b> | N146T          |   |   | N146A                            |                                       | N146F                            |                        |                                   |
| <b>K147</b> |                |   | K147R<br>K147Q  |                                  |                                       |                                  |                        |                                   |
| <b>R148</b> |                | R148G   | R148K<br>R148V  |                                  | R148P                                 | R148L<br>R148Q<br>R148E          | R148K                  |                                   |
| <b>T149</b> | T149G<br>T149R | T149A<br>T149E<br>T149Q                                   |   | T149V<br>T149M<br>T149W          | T149P                                 |                                  |                        |                                   |
| <b>P150</b> |                |   | P150R<br>P150N<br>P150D<br>P150G<br>P150I<br>P150L<br>P150F<br>P150S<br>P150T |                                  |                                       |                                  | P150D                  | P150T<br>P150N<br>P150L<br>P150G  |
| <b>R151</b> |                | R151A<br>R151T  |   | R151Q<br>R151M<br>R151L<br>R151K |                                       |                                  |                        |                                   |
| <b>R152</b> |                |   |   | R152V<br>R152A                   |                                       | R152N<br>R152P<br>R152D          |                        |                                   |

Fig. 1

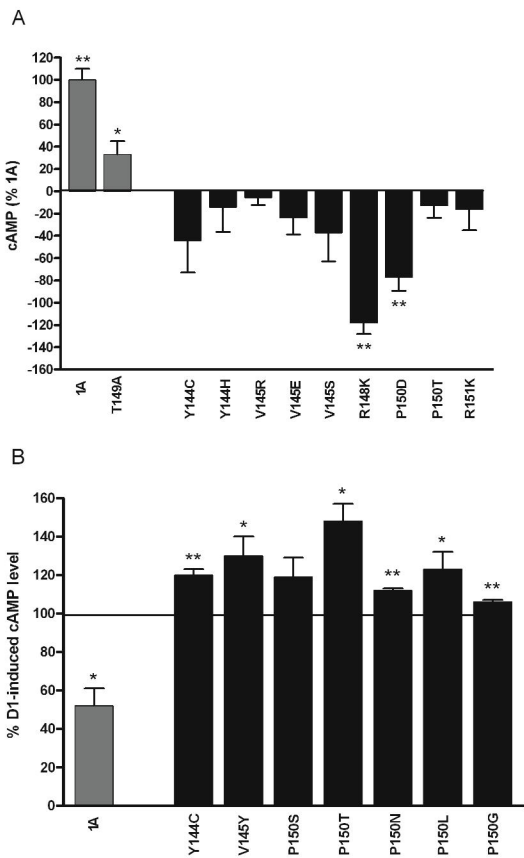
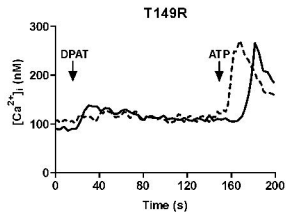
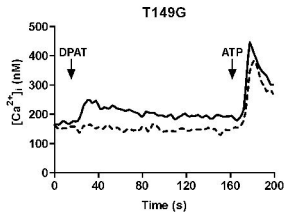
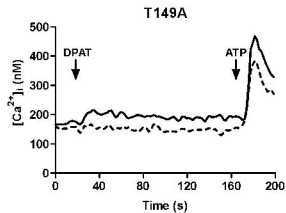
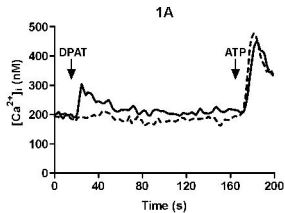


Fig. 2



**Figure 3**

